Simulation and analysis of ice-induced vibrations experienced but Molikpaq during the May 12, 1986 event

Owen, C.C.; Hendrikse, H.

Publication date
2021

Document Version
Final published version

Published in
Proceedings of the 26th International Conference on Port and Ocean Engineering under Arctic Conditions

Proceedings of the 26th International Conference on
Port and Ocean Engineering under Arctic Conditions
June 14-18, 2021, Moscow, Russia

Simulation and analysis of ice-induced vibrations experienced by Molikpaq during the May 12, 1986 event

Cody C. Owen[1], Hayo Hendrikse[1]
[1] Delft University of Technology, Delft, The Netherlands

ABSTRACT

Much attention has been given to the dynamic ice-structure interaction of the Molikpaq caisson which resulted in severe, almost catastrophic, structural vibrations during the winter of 1985-1986 at Amauligak I-65 in the Canadian Beaufort Sea. In this study, specific focus is given to the scientific literature describing the ice-induced vibration event on May 12, 1986 over the observed range of ice conditions and drift speeds. While considering the limitations of the measurement data available for the event, the scenario is reviewed and a recent phenomenological model is implemented to simulate the ice-induced vibrations observed. A simplified model of the Molikpaq caisson is simulated to interact with an ice floe and the results are compared with the full-scale observations from the event. Limitations of the modeling with respect to the available full-scale data are discussed and modeling results are compared to previous simulations attempting to explain the event on May 12, 1986. It is concluded that this ice-induced vibration event should be treated with caution and detailed considerations of the scenario, including a comprehensive structural model, must be implemented for accurate simulation of the event on May 12, 1986. Models and theories derived exclusively from this event should be scrutinized in light of its uncertain and complex conditions and thus treated skeptically.

KEY WORDS: Intermittent crushing, ice floe, brittle crushing

INTRODUCTION

The Molikpaq caisson—a steel, octagonal annulus filled with a sand core and placed on an underwater sand berm—experienced severe ice-induced vibrations while stationed at Amauligak I-65 in the Beaufort Sea during the 1986 spring season (Jefferies and Wright, 1988). The most comprehensive ice-induced vibration event from this structure, which occurred on May 12, 1986, was captured with an array of load panels, strain gauges, accelerometers, and extensometers, in addition to numerous geotechnical recordings and detailed visual observations (Timco and Johnston, 2003). However, significant uncertainty in the measurements renders this ice-induced vibration case challenging to quantify. In this study, the dynamic interaction between the Molikpaq and a large ice floe is simulated while considering the vast uncertainties in the site conditions and measurements during the event. An envelope of site conditions and structural properties is developed to determine whether this event can be simulated by the proposed ice model and what conclusions can be drawn about the largest and arguably the most prominent ice-induced vibration event ever recorded.

DESCRIPTION OF THE MOLIKPAQ

The mobile arctic caisson called Molikpaq comprises three main parts: 1) the octagonal annular caisson made of steel bulkheads and frames with a simply supported steel deck; 2) the sand core retained inside the caisson; and 3) the sand berm upon which the sand core and the caisson were stationed. At the waterline at this site, the Molikpaq had main faces with lengths reported between 58 m and 60 m, and corner faces with lengths of 22 m, and all of these faces had a slope of about 7° or 8° from vertical (Timco, Johnston and Wright, 2005; Jefferies, 2010; Jordaan, Hewitt and Frederking, 2018). The sand core had dimensions of 72 by 72 m (or 73 by 73 m (Jefferies and Wright, 1988)) with a depth of about 21 m (Jordaan, Hewitt and Frederking, 2018), and was later reviewed to have a loose state of sand (Hewitt, 2011). The sand berm was described as having stiff and dense sand (Jefferies, 2010). During ice loading on the caisson, the load was transferred to the sand berm via base friction and into the sand core, which was then transferred to the berm. The ratio of base shear to sand core resistance during dynamic interaction is debated in literature (Jordaan, Hewitt and Frederking, 2018).

Instrumentation

External ice loads acting on the Molikpaq were measured by 30 (later clarified as 31 (Timco and Johnston, 2003)) MEDOF load panels that were placed in a total of seven clusters on the north, northeast, and east faces of the caisson and covered about 10% of the nominal ice-structure interface contact area (Jefferies and Wright, 1988). 28 of the 31 panels were functional during the 1985-1986 ice season (Jordaan, Hewitt and Frederking, 2018). Each panel was 2.715 m tall and 1.135 m wide and the top of the middle panels were located at the waterline, which permitted estimation of ice thickness based on load readings from the middle and bottom panels. The panels were calibrated for pressures up to 1.86 MPa, and were sensitive to temperature and demonstrated creep development rapidly (Jordaan, Hewitt and Frederking, 2018). It is very likely that the ice floe imparted greater pressures than the maximum calibration pressure, which is evidenced by the saturation load observed on load panel N2_1010 during the May 12 event (Timco, Johnston and Wright, 2005; Sudom and Frederking, 2010). This supports the analysis which concludes that the MEDOF load panels overestimated the loads by as much as a factor of 2 during loading events in the 1985-1986 ice season (Jordaan, Hewitt and Frederking, 2018). This has implications for the loads derived from extensometer and strain gauge data which were calibrated with the MEDOF panel measurements, the loads from which had to be upscaled to the interaction width since the perimeter of the structure was not completely covered with load panels (Jefferies *et al.*, 2011). The most important limitation of the load panels was the response time of 5 to 10 s, and frequencies above 0.5 Hz were likely missed by the load measurements (Jefferies and Wright, 1988; Frederking and Sudom, 2006). In effect, the load panels could only measure slow-varying mean ice loads during dynamic ice-structure interaction.

Strain gauges were installed in the upper struts of the main bulkheads of the caisson near the load panels (Jefferies, 2010). Similarly, accelerometers were located at the base and deck levels of the caisson in a vertically in line with the strain gauges. Extensometers were installed between the caisson and the box girder deck, which was simply supported by the caisson and rested on rubber bearings. The extensometers measured the ovalling or ring distortion of the caisson and could be used to estimate the deflection of the caisson face subjected to ice loading. The strain gauges, accelerometers, and extensometers had a sampling frequency of 50 Hz during burst file recordings. Although the burst file recordings had a sampling rate of 50 Hz, the anti-aliasing low-pass filter utilized in the data acquisition system filtered out signals above 20 Hz and reduced amplitudes of lower frequencies in an undesirable manner (Spencer,

Morrison and Jefferies, 2011). Furthermore, measurements from the strain gauges, accelerometers, and extensometers measured the structural response and not the ice load, implying that any high frequency content in the ice load is assumed to be filtered by the structure even before being measured, depending on the locations and sensitivity of the instruments.

Dynamic structural properties

The Molikpaq is a complex structure and requires a detailed structural model to describe the response to multi-directional dynamic loading (Brown *et al.*, 1992; Morsy and Brown, 1996); however, this information is not readily available. Instead, the public data are collected and a single-degree-of-freedom oscillator is roughly approximated to describe the structure in the dynamic ice-structure interaction scenario. The total horizontal translation of the structure was described as having a natural frequency of 1.3 Hz and modal stiffness of 67 GN m^{-1}, and the loaded wall showed a natural frequency of 5.6 Hz and modal stiffness of 180 GN m^{-1} (Jefferies and Wright, 1988; Brown *et al.*, 1992). A natural frequency of 1.26 Hz, damping ratio as fraction of critical of 20%, and a global stiffness of 10 GN m^{-1} were offered in the Joint Industry Project (JIP) on ice-induced vibrations (Kärnä *et al.*, 2013). However, a north-south extensometer calibration stiffness of between 2.3 GN m^{-1} and 2.8 GN m^{-1} was found to be necessary for the floe to decelerate to a stop against the Molikpaq in about 27 minutes (Fuglem, Jordaan and Bruce, 2011). Morsy and Brown (1996), in their model of the Molikpaq, considered system damping between 10 and 20% of critical, which is in accordance with the value chosen for the JIP.

SITE CONDITIONS

On May 12, 1986, a floe of first-year sea ice with multi-year inclusions and rectangular dimensions of 4 nmi by 8 nmi (approximately 7 km by 15 km) crushed against primarily the north face Molikpaq with an initial speed of 0.2 m s^{-1} and decelerated to a stop against the structure (Jefferies and Wright, 1988). The interaction began at 03:01 and ended at 03:26. Approximately 162 m of ice crushed against the structure over the course of the event (Sudom and Frederking, 2010). Later reviews specified an initial floe speed of 0.18 m s^{-1} and crushing against both the north and northeast faces of the Molikpaq, and full contact was apparently reached at 03:10 (Timco, Johnston and Wright, 2005). It is debated whether full contact with the north face happened until at least 03:12, and the average load did not become relatively steady until about 03:19 (Gagnon, 2012). At around 03:19, the approximate floe speed was 0.09 m s^{-1} (Jefferies, 2010). The first-year ice was estimated by visual observation as 1.7 to 2 m thick with possible multi-year inclusions of up to 4 m thickness, and during the interaction one of the lower MEDOF panels recorded loading, which suggested between 2.8 and 5 m of ice thickness (Timco, Johnston and Wright, 2005; Jefferies, 2010). At 03:24 during the interaction, a crack formed near the western end of the north face which led to a wedge of the floe breaking away, leaving the northwest face free from ice (Jefferies, 2010).

The first-year ice was noted to have a thickness of 1.8±0.5 m, which is consistent with previous reports, and the event was stated to have lasted overall from 03:00 to 03:30 (Jefferies, 2010). However, it was corrected that the ice thickness likely ranged from 2 to 3 m during the event due to load measurements from the lower load panels on the north and northeast faces which probably experienced ice thicknesses of 3.3 m and 2.8 m, respectively. During the event, ice rubble piles along the upper ice-structure interface were estimated to be a maximum of 8 m high and 10 m wide, which implied ice thickness of about 2 m from video inspection (Sudom and Frederking, 2010). It is mentioned that an ice crushing pressure of 1.4 MPa was estimated based on an ice thickness of 2.8 m when the lower load panel recorded a load during the third

burst file of the event (Jefferies, 2010). The highest global pressure measured on the Molikpaq was 1.8 MPa for first-year level ice, although most global pressures were less than 1.5 MPa (Timco and Johnston, 2003). It is important to note that the floe decelerated in a nonlinear manner, and decelerated rapidly during the final 5 min of interaction (Jefferies, 2010; Gagnon, 2012). The wind speed in the general direction of the ice floe motion at initial contact was measured as 6.2 m s^{-1}, and an initial current speed in the general direction of ice floe motion was assumed to be 0.09 m s^{-1} (Fuglem, Jordaan and Bruce, 2011).

Also of interest to this study is the observation of plastic deformation of the sand core and/or caisson at the northeast face and eastern portion of the north face on the order of 14 mm as indicated by the inclinometers, extensometers, and strain gauges during and after the event (Rogers, Spencer and Hardy, 1991; Hardy *et al.*, 1998). This plastic deformation appeared to have occurred during the latter part of the interaction when dynamics played a significant role and sustained ice loads of at least 150 MN could be extrapolated from the load panels.

INTERACTION SCENARIO

It is well documented that this ice-induced vibration event involved a massive, isolated floe which crushed against a wide structure, which under normal ice conditions would be considered stiff, and decelerated to a halt. Even with the load identification, filtering, and sampling rate limitations of the data, it was confidently reported that a transition from non-simultaneous to simultaneous crushing during ice-structure interaction occurred in several instances (Jefferies and Wright, 1988; Jefferies, 2010). Dissenting views assert that transition from non-simultaneous to simultaneous crushing of the ice sheet against the structure did not play a role in the ice-induced vibrations of the Molikpaq during the event (Gagnon, 2012). However, this assertion is made using an absence of evidence and faults the data acquisition limitations as an excuse for this absence of reliable evidence.

Ice model

The phenomenological ice model implemented for this study is illustrated in Figure 1 and described in detail in Hendrikse and Nord (2019). The ice floe and crushing aspects of the model are one-dimensional, and do not include rotation or bending and buckling failure modes of the floe during interaction. The reference parameters to define the ice behavior are given in Hendrikse and Nord (2019) and are reproduced in Table 1. The scaling approach from reference input parameters to other parameters, such as structure width, is discussed elsewhere (Hendrikse, Ziemer and Owen, 2018). It is emphasized that these reference parameters were derived from the STRICE campaign data from the Norströmsgrund lighthouse in the northern Baltic Sea. The Baltic Sea ice is strictly first-year ice with potential first-year inclusions such as rafted or ridged ice, and has a lower salinity than that of Beaufort Sea ice. Although the differences in the physical properties between Baltic Sea and Beaufort Sea ice are quantifiable, their impact on the ice-induced load on their respective structures is not well understood. Thus, in this case, the potential differences are grouped into the uncertainty in the ranges of ice thickness and strength values considered for the simulations. In addition, the parameters for defining the Beaufort Sea ice floe are given in Table 2.

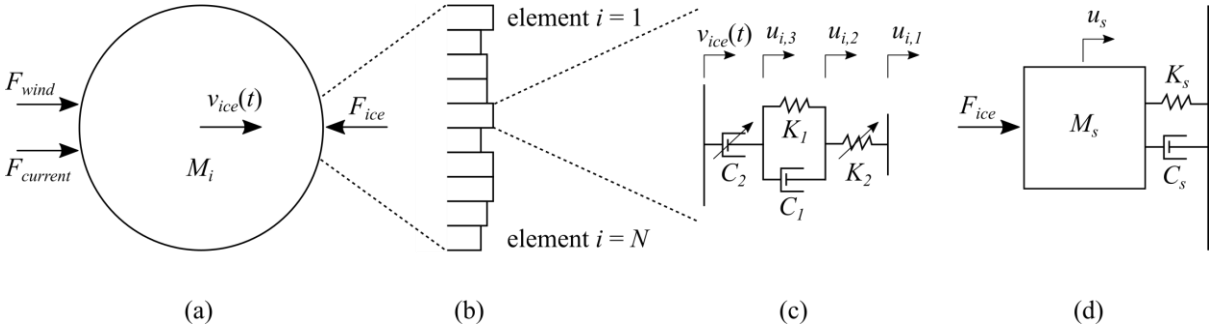

Figure 1. Illustration of the ice model comprising a) an equivalent ice floe with wind and current driving forces; b) an ice edge with N ice elements; c) each ice element as a nonlinear Burgers model with Kelvin representation; and d) a single-degree-of-freedom oscillator representation of the structure. A detailed description of the ice model is given by Hendrikse and Nord (2019).

Table 1. Reference input parameters from northern Baltic Sea ice for the ice model derived from STRICE campaign data from the Norströmsgrund lighthouse with diameter of 7.5 m and 3.5 MN mean brittle crushing load (Hendrikse and Nord, 2019). Note that the dashpot $C_{2,ref}$ is nonlinear with a cubic power.

$K_{2,ref}$ [N m^{-1}]	$C_{2,ref}$ [N^3 m^{-1} s]	$K_{1,ref}$ [N m^{-1}]	$C_{1,ref}$ [N m^{-1} s]	N_{ref} [-]	$r_{max,ref}$ [m]	$\delta_{f,ref}$ [m]
$5.28 \cdot 10^7$	$4.71 \cdot 10^{18}$	$1.38 \cdot 10^7$	$4.96 \cdot 10^7$	58	$6 \cdot 10^{-3}$	$4 \cdot 10^{-3}$

Table 2. Ice floe parameters for the ice model to simulate the May 12, 1986 event (Fuglem, Jordaan and Bruce, 2011).

ρ_i [kg m^{-3}]	A_i [m^2]	ρ_w [kg m^{-3}]	$C_{d,w}$ [-]	ρ_a [kg m^{-3}]	$C_{a,w}$ [-]	v_w [m s^{-1}]	v_a [m s^{-1}]
920	$105 \cdot 10^6$	1027	$2.5 \cdot 10^{-3}$	1.29	$1.9 \cdot 10^{-3}$	0.09	6.2

Simulation parameters

The input parameters to the ice model for the simulations are shown in Table 3. Given the uncertainty in the modal properties of the structure, it is assumed that crushing only occurs on the north face of the structure with approximate width d of 60 m. Similarly, the fundamental frequency f_s of the structure, namely in translational deflection, is approximated as 1.3 Hz. As for the dynamic stiffness K_s of this deflection, which includes the caisson and sand core, 10 GN m^{-1} is selected. The structural damping as a fraction of critical damping ζ_s is estimated as 20%. The structure is assumed to have negligible initial waterline displacement $u_{s,0}$ and velocity $\dot{u}_{s,0}$ at the start of every simulation. A wide range of ice thicknesses were observed in the floe, and the measurement methods of visual observation and panel activity allow for large error in the actual ice thicknesses that crushed against the structure. Moreover, the compressive strength of the ice during this event varied considerably throughout the floe, depending on whether the ice was first-year or multi-year. Therefore, an envelope of lower and upper bound estimates for ice thickness h and compressive strength σ are estimated for simulation, which includes two specific cases near the median of these values for comparison with the full-scale

data of the event. Although the interaction apparently involved a width of 89 or 90 m (Sudom and Frederking, 2010; Jefferies *et al.*, 2011), the load attributed to this wider interaction is incorporated in the envelope of ice conditions via thicker and stronger ice (which ignores aspect ratio effects and complex structural deflections). Moreover, the interaction width of 60 m is selected because 1) the majority of in-line dynamic interaction was reported to have occurred with the north face; and 2) this width was also considered for another numerical ice model (Gagnon, 2020).

The dynamic ice-structure interaction event is performed as a time domain simulation with the floe as specified in Table 2. Each of the simulations is executed for 800 s or until the floe is arrested. The floe is assumed to begin with an initial speed of 0.09 m s^{-1} to account for the instant when there was complete ice-structure contact and the mean brittle crushing load was relatively steady during the event. All of the simulations are completed with an output time step of 0.02 s (equivalently 50 Hz sampling rate).

Table 3. Input parameters to the ice model for simulation of the May 12, 1986 event with the Molikpaq.

Trial name	d [m]	f_s [Hz]	K_s [N m^{-1}]	ζ_s [%]	h [m]	σ [Pa]	$u_{s,0}$ [m]	$\dot{u}_{s,0}$ [m s^{-1}]
T1 (lower)	60	1.3	$10 \cdot 10^9$	20	1.3	$1 \cdot 10^6$	0	0
T2 (case 1)	60	1.3	$10 \cdot 10^9$	20	2.3	$1.1 \cdot 10^6$	0	0
T3 (case 2)	60	1.3	$10 \cdot 10^9$	20	2.5	$1.4 \cdot 10^6$	0	0
T4 (upper)	60	1.3	$10 \cdot 10^9$	20	3.3	$2 \cdot 10^6$	0	0

SIMULATION RESULTS

Overview

The simulation results (T1-T4) for the dynamic ice-structure interaction between the Molikpaq and the decelerating floe for a range of ice thicknesses and strengths are shown in Figure 2. The lower bound case (T1) results in the lowest loads and structural responses and the longest duration of interaction. This is expected as the load acting on the floe is lowest and least resists the momentum and driving forces acting on the floe. The specific cases (T2-T3) result in moderate loads and structure responses and moderate duration. The upper bound case (T4) results in the highest loads and structure responses and the shortest duration of interaction. For all four cases, the floe deceleration is approximately constant until significant dynamic ice-structure interaction develops, which causes the floe to decelerate rapidly to a halt. Specifically, continuous brittle crushing dominates until the floe velocity reaches roughly 0.01 m s^{-1} for T1, 0.02 m s^{-1} for T2 and T3, and 0.03 m s^{-1} for T4, below which intermittent crushing vibrations govern the interaction until the floe nearly stops and ductile deformation occurs at the very end of the interaction (observed as the smooth final peak in the global ice load time histories).

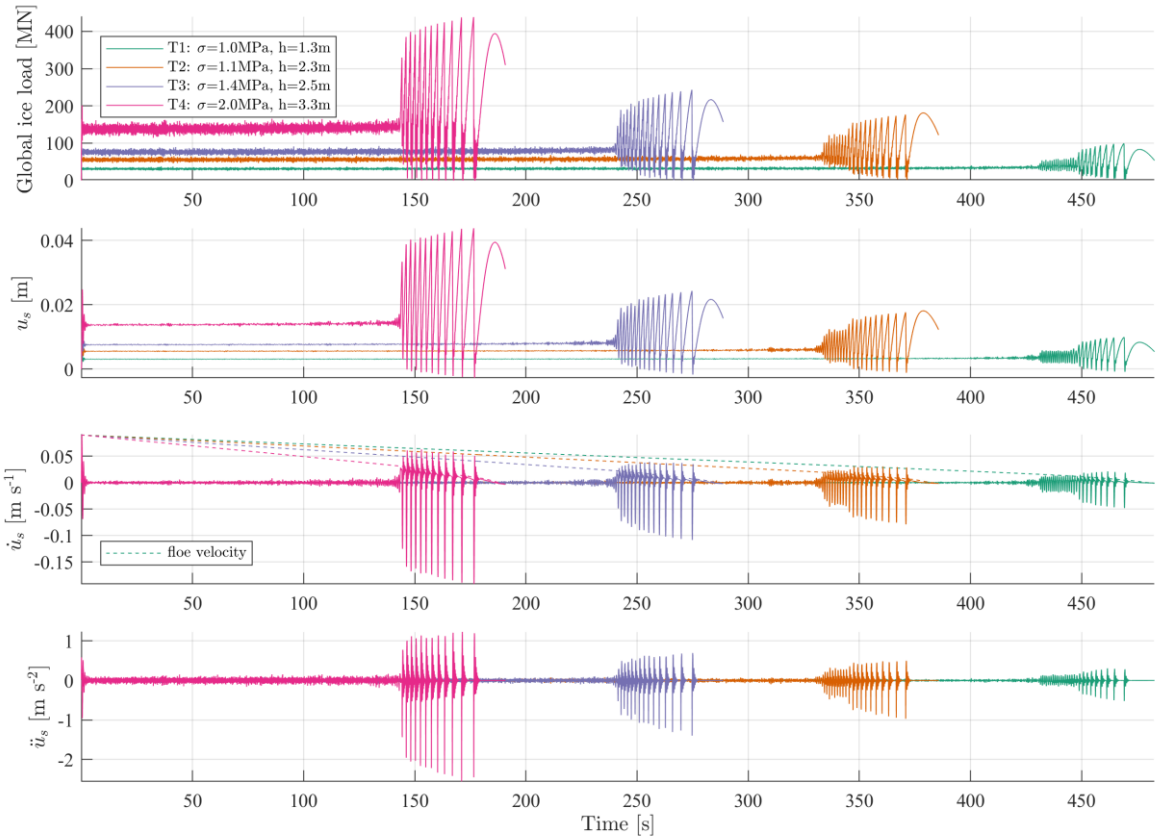

Figure 2. Simulations (T1-T4) of dynamic ice-structure interaction between the Molikpaq and decelerating floe with range of ice thicknesses and compressive strengths from the May 12, 1986 event.

Signal filtering

Knowing that the anti-aliasing filtering had a deleterious effect on the measured signals, a similar filter (low-pass, flat top window FIR filter with order 18 and cutoff frequency of 7 Hz) is applied to case 1 (T2) and compared with the unfiltered signal from the simulation results (see Figure 3). But, in order to compare the global load from the simulation results to that from the measurements, it has to be highlighted that the global loads from the structure were measured by load identification via calibrated extensometers and strain gauges. Thus, the simulated global load is derived from the structural displacement in the model by taking the product of the displacement and an effective stiffness, that being the quasi-static ratio between the peak from the global ice load and the corresponding peak structural displacement during intermittent crushing. Following this procedure, the simulated identified global ice load and acceleration time histories are shown in Figure 3 and the simulated identified global ice load is compared with the simulated global ice load directly from the model. It can be seen that the structure, especially when treated as a single-degree-of-freedom oscillator, filters the high frequency content from the load signal. The identified global load shows negative, and thus unphysical, values due to the inertia of the structure rebounding after the rapid load drops; ice-induced global loads would otherwise not drop below zero. In accordance with Spencer et al. (2011), the anti-aliasing filter significantly attenuates the initial peaks of the acceleration signal succeeding the global load drops.

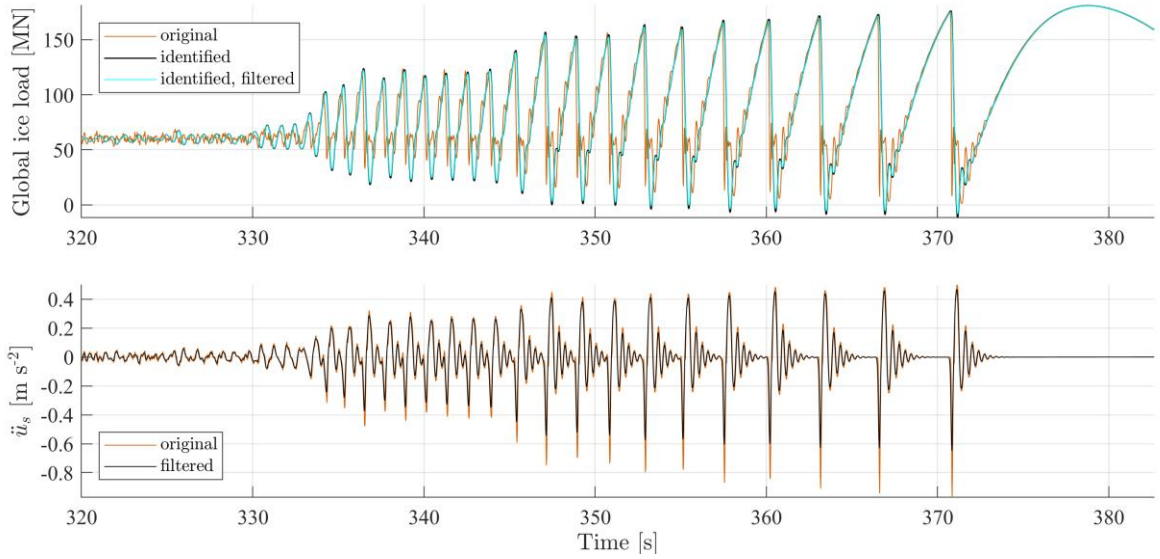

Figure 3. Simulated global ice load (original) and structural acceleration (original) time histories (T2) from model with and without anti-aliasing filtering. The simulated identified global ice load (identified) is derived from the product of the structural displacement and an effective stiffness.

DISCUSSION

The simulated results when compared to the May 12, 1986 event show good qualitative agreement in terms of the types of and transitions between mechanisms of interaction. The transition from non-simultaneous to simultaneous failure and synchronization of the fundamental frequency of the Molikpaq with the global ice load is captured by the model. The transition from intermittent crushing to ductile deformation as the ice comes to a stop near the end of the event is also captured by the ice model. Quantitatively, the envelope of interactions contains the measured loads, deflections, and accelerations observed during the event. However, the exact values of those measurements are not matched by the model; this can be accounted for by a myriad of reasons. First, the structure is oversimplified to a single-degree-of-freedom representation, which misses many aspects of the interaction, including loaded wall and torsion modes (Morsy and Brown, 1996), and ice action on the corner faces and shear on the side faces (Sudom and Frederking, 2010). This representation allocates too much stiffness to the first mode and not to the other modes which must participate in the dynamic interaction. This assumption appears rather erroneous because other modes of the structure are clearly observed in the extensometer and accelerometer measurements during the event (Timco, Johnston and Wright, 2005) and detailed finite element modelling of the Molikpaq caisson, core, and berm suggest that the first 10 modes all have natural frequencies below 3 Hz (Morsy and Brown, 1996) and many other natural frequencies lie below 6 Hz (Brown *et al.*, 1992). Furthermore, the frequencies present in the acceleration signals from the first (Kärnä *et al.*, 2013) and second (Timco, Johnston and Wright, 2005) burst files indicate higher modes acting in the interaction, modes other than that of the natural frequency chosen for the simulations that was present in the extensometer readings (Timco, Johnston and Wright, 2005). This further supports the claim that the oversimplification of the structure cannot properly capture the structural response during the dynamic ice-structure interaction and that a more descriptive structural model is needed to accurately reproduce the measurements from the event.

One of the few quantitative observations that can be readily compared to the simulated results

is the floe deceleration with respect to change in floe velocity during the burst file measurements. The floe had a speed of 0.09 m s^{-1} at 03:20, was moving at about 0.072 m s^{-1} after 120 s, and was moving at roughly 0.006 m s^{-1} after 325 s (Jefferies, 2010). These floe velocities at their corresponding times are contained within the envelope of simulated results, and fit between the lower bound case (T1) and case 1 (T2).

The global ice load time histories from the simulated results, when directly compared to those from either the calibrated strain gauge data or extensometers north face data (with plastic deformation removed) from DynaMAC (Hardy *et al.*, 1998; Kärnä *et al.*, 2013), appear unsatisfactory (see Figure 4). Most salient are the disparity in the mean brittle crushing load and the ratio between peak loads in intermittent crushing and in continuous brittle crushing. It is, nevertheless, important to recognize that the ice thickness and strength varied significantly during the event, and an ice wedge on the northwest face broke away from the interaction just before 03:24, which contributed to the time-varying mean load observed in the data (Jefferies, 2010). The large difference in mean displacements between the simulations and measurements might be accounted for not only by the structure simplification, but also by the load-dependent nonlinear structural deflection that was investigated by numerical modelling with respect to the extensometer calibration (Rogers, Spencer and Hardy, 1991). Based on the comparison between the acceleration time histories, the structure response is tolerable but reinforces the fact that the oversimplification of the structure causes the transient responses to be larger than measured during intermittent crushing.

Uncertainty in the reported ice conditions originates from the variability in local ice thicknesses and strengths distributed throughout the ice floes, including ridges and multi-year inclusions. The reference measurements from the Norströmsgrund lighthouse reference case incorporated to some extent these kinds of variations implicitly (Nord, Petersen and Hendrikse, 2019), which means that local variations cannot be identified and separated from the derived ice parameters. In effect, this limits the applicability of the Norströmsgrund lighthouse reference case to the May 12, 1986 event on the Molikpaq because these local variations are demonstrably different between the Norströmsgrund lighthouse and Molikpaq cases with rather different ice types and formative conditions. Moreover, the statistical properties derived from the STRICE data appear unsuitable for the scaling between the two structures based on the ratio between the global ice load mean and maximum as seen in Figure 4.

Besides the complexity of the structure and the floe interaction, ice rubble above and below the intact ice floe and its effect on the mean brittle crushing load undoubtedly contributed to the interaction (Sudom and Frederking, 2010) but are not included in the ice model. It is inferred that the ice rubble static component in the global ice load would increase the mean brittle crushing load, but should not increase the maximum loads associated with dynamic interaction or the standard deviation. Essentially, the ice rubble would increase the mean load such that the global ice load would not drop to near zero during intermittent crushing and the ratio between peak load during intermittent crushing and mean load during brittle crushing would decrease. However, the maximum static load from ice rubble would only be about 10% of the brittle crushing mean load, and therefore would not alone account for the difference between the simulated and measured global loads (Kärnä and Yan, 2009).

In contrast to this study, the event has been simulated with a detailed structural model but limited dynamic ice-structure interaction (Morsy, 1995; Morsy and Brown, 1996). The time domain simulations with an ice floe were performed only for a few seconds due to computational limitations but showed initial promise by modeling the ice with a Burgers element for intact damaged ice and stick-slip viscous element for the crushed ice. The event

has also been simulated by assuming a spallation mechanism with uniform spalling depths and purely linear elastic ice behavior apart from nonlinear deformation at the ice-structure interface (Gagnon, 2020). A static load component of 100 MN from crushed ice, like ice rubble, is assumed to act on the structure. Each spall is defined with a depth of 0.054 m and a width of 60 m, the full interaction width which necessarily precludes any non-simultaneous ice failure behavior. The crushable foam definition of the process surface has a nonlinear elastic stress-strain relationship which is fit such that the change of 127 MN in the sawtooth loads emulates that from measurements. The intermittent crushing vibrations are captured by the numerical model, but only by prescribing a spalling length and ice floe speed which result in sawtooth load patterns at or below the natural frequency of the single-degree-of-freedom representation of the Molikpaq structure. The at-spallation-resonant-frequency termed by Gagnon (2020) does not involve resonance but actually refers to the transient response of the structure after rapid unloading that is superimposed on the load buildups which are caused by the anelastic behavior of the ice.

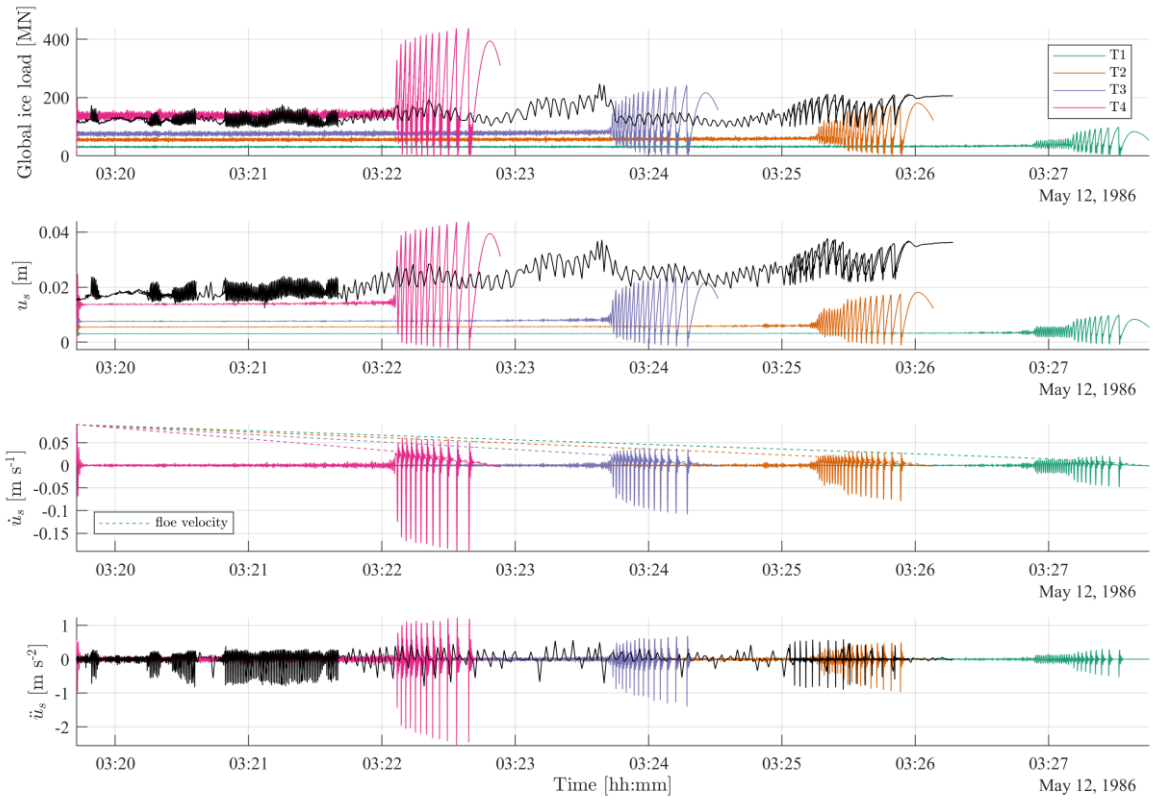

Figure 4. The simulated results from Figure 2 compared with the identified global ice loads (from strain gauges), extensometer deflections, and accelerations (all shown in black) from the fast and three burst files superimposed from the May 12, 1986 event. Note that the three burst files data are superimposed on the fast file data to show signal consistency between the different sampling rates.

CONCLUSION

The May 12, 1986 event between the Molikpaq and a massive first-year ice floe with multi-year inclusions resulted in egregious structural vibrations and detailed research as to the explanation of such ice-induced vibration. Based on the available data on floe size, initial floe speed, driving forces, ice thickness and strength, and structure properties, the dynamic

interaction between the Molikpaq and the decelerating floe can be simulated with the phenomenological ice model to show an envelope of adequate qualitative results, but the exact measurements cannot be replicated without fitting, e.g. arbitrarily adding a static load component as performed in other models. Crucially, the model captures well the transition from non-simultaneous to simultaneous ice failure and synchronization of the fundamental frequency of the Molikpaq with the global ice load. The amount of uncertainty in all of the aforesaid parameters, and the proprietary load identification and calibration techniques used for the global loads from strain gauge and extensometer data, make accurate simulation of the event extremely difficult to attain. Development of a detailed structural model for the Molikpaq would offer better simulated results, but ultimately the uncertainty in the ice conditions and structural properties makes accurate simulation of this event an unwieldy and possibly futile task. It is concluded that this ice-induced vibration event should be treated with caution and detailed considerations of the scenario, including a comprehensive structural model, must be implemented to attempt an accurate simulation of the event on May 12, 1986. Models and theories derived exclusively from this event should be scrutinized in light of its uncertain and complex conditions and thus treated skeptically.

ACKNOWLEDGEMENTS

The authors thank the participating organizations in the SHIVER project: TU Delft, Siemens Gamesa Renewable Energy, and Aalto University, for supporting this work. The SHIVER project is co-financed by Siemens Gamesa Renewable Energy and TKI-Energy by the 'Toeslag voor Topconsortia voor Kennis en Innovatie (TKI's)' of the Dutch Ministry of Economic Affairs and Climate Policy.

REFERENCES

Brown, T. G. *et al.* (1992) 'A model for dynamic ice interactions with Molikpaq', in *Proceedings of the 11th IAHR International Symposium on Ice*. Banff, Alberta, Canada: IAHR, pp. 1289–1303. Available at: https://www.iahr.org/index/committe/14.

Frederking, R. and Sudom, D. (2006) 'Maximum ice force on the Molikpaq during the April 12, 1986 event', *Cold Regions Science and Technology*, 46(3), pp. 147–166. doi: 10.1016/j.coldregions.2006.08.019.

Fuglem, M., Jordaan, I. and Bruce, J. (2011) 'Estimation of the peak impact load on the Molikpaq by a multi-year floe on May 12, 1986 based on floe deceleration', in *Proceedings of the 21st International Conference on Port and Ocean Engineering under Arctic Conditions*. Montréal, Canada: POAC, pp. 1–12.

Gagnon, R. (2020) 'Spallation-Based numerical simulation of ice-induced vibration of a structure', in *Proceedings of the 25th International Symposium on Ice*. Trondheim, Norway: IAHR, pp. 1–11. Available at: https://www.researchgate.net/publication/347974341_PROCEEDINGS_OF_THE_25th_INTERNATIONAL_SYMPOSIUM_ON_ICE.

Gagnon, R. E. (2012) 'An explanation for the Molikpaq May 12, 1986 event', *Cold Regions Science and Technology*. Elsevier B.V., 82, pp. 75–93. doi: 10.1016/j.coldregions.2012.05.009.

Hardy, M. D. *et al.* (1998) *DynaMAC: Molikpaq ice loading experience*. Calgary, Alberta, Canada.

Hendrikse, H. and Nord, T. S. (2019) 'Dynamic response of an offshore structure interacting with an ice floe failing in crushing', *Marine Structures*, 65, pp. 271–290. doi: 10.1016/j.marstruc.2019.01.012.

Hendrikse, H., Ziemer, G. and Owen, C. C. (2018) 'Experimental validation of a model for prediction of dynamic ice-structure interaction', *Cold Regions Science and Technology*, 151, pp. 345–358. doi: 10.1016/j.coldregions.2018.04.003.

Hewitt, K. (2011) 'Ice loads on the Molikpaq at Amauligak I-65 based on geotechnical analyses and responses', in *Proceedings of the 21st International Conference on Port and Ocean Engineering under Arctic Conditions*. Montréal, Canada: POAC, pp. 1–13.

Jefferies, M. (2010) *Molikpaq dynamic ice-structure interaction at Amauligak 1985-6: measurements & data*. 11179. Oslo, Norway.

Jefferies, M. *et al.* (2011) 'Ice load measurement on Molikpaq: methodology and accuracy', in *Proceedings of the 21st International Conference on Port and Ocean Engineering under Arctic Conditions, POAC*. Montréal, Canada: POAC, pp. 1–13.

Jefferies, M. G. and Wright, W. H. (1988) 'Dynamic response of Molikpaq to ice-structure interaction', *Proceedings of the 7th International Conference on Offshore Mechanics and Arctic Engineering*, IV, pp. 201–220.

Jordaan, I., Hewitt, K. and Frederking, R. (2018) 'Re-evaluation of ice loads on the molikpaq structure measured during the 1985–86 season', *Canadian Journal of Civil Engineering*, 45(3), pp. 153–166. doi: 10.1139/cjce-2016-0444.

Kärnä, T. *et al.* (2013) 'Ice-induced vibrations of offshore structures - looking beyond ISO 19906', in *Proceedings of the 22nd International Conference on Port and Ocean Engineering under Arctic Conditions*. Espoo, Finland: POAC, pp. 1–12. Available at: http://www.poac.com/PapersOnline.html.

Kärnä, T. and Yan, Q. (2009) *Analysis of the size effect in ice crushing - edition 2*. Espoo/Helsinki, Finalnd.

Morsy, U. A.-E. (1995) *Non-linear finite element modelling of dynamic loads on offshore structures*. University of Calgary. doi: http://dx.doi.org/10.11575/PRISM/15646.

Morsy, U. A. and Brown, T. G. (1996) 'Three-dimensional non-linear finite element model for the Molikpaq, Gulf's mobile caisson', *Computers & Structures*, 60(4), pp. 541–560. doi: 10.1016/0045-7949(95)00430-0.

Nord, T. S., Petersen, Ø. W. and Hendrikse, H. (2019) 'Stochastic subspace identification of modal parameters during ice–structure interaction', *Philosophical Transactions of the Royal Society A: Mathematical, Physical and Engineering Sciences*, 377(2155), p. 20190030. doi: 10.1098/rsta.2019.0030.

Rogers, B. T., Spencer, P. A. and Hardy, M. D. (1991) *Dynamic ice/structure interaction with the Molikpaq at Amauligak I-65; Phase 2, Vol. 2 of 2 - Load measurement on the Molikpaq at Amauligak I-65*. CHC 14-24.

Spencer, P., Morrison, T. and Jefferies, M. (2011) 'The effect of low pass filters in the Molikpaq data acquisition system on "phase lock" interaction signals', in *Proceedings of the 21st International Conference on Port and Ocean Engineering under Arctic Conditions, POAC*. Montréal, Canada: POAC, pp. 1–10.

Sudom, D. and Frederking, R. (2010) 'A closer examination of the May 12, 1986 ice floe impact with the Molikpaq', *International Conference and Exhibition on Performance of Ships and Structures in Ice 2010, ICETECH 2010*, (122), pp. 361–368. Available at: https://www.researchgate.net/publication/289344415_A_closer_examination_of_the_May_12

_1986_ice_floe_impact_with_the_Molikpaq.

Timco, G. . and Johnston, M. (2003) ‘Ice loads on the Molikpaq in the Canadian Beaufort Sea’, *Cold Regions Science and Technology*, 37(1), pp. 51–68. doi: 10.1016/S0165-232X(03)00035-1.

Timco, G. W., Johnston, M. E. and Wright, B. D. (2005) ‘Multi-year ice loads on the molikpaq: May 12, 1986 event’, in *Proceedings of the 18th International Conference on Port and Ocean Engineering under Arctic Conditions*. Potsdam, New York, USA: POAC, pp. 453–462. Available at: http://www.poac.com/PapersOnline.html.